Journal of Colloid and Interface Science 434 (2014) 152–158

Contents lists available at ScienceDirect

Journal of Colloid and Interface Science

www.elsevier.com/locate/jcis

Fast adsorption of Cd^{2+} and Pb^{2+} by EGTA dianhydride (EGTAD) modified ramie fiber

Zhichao Sun, Yunguo Liu *, Yuanqing Huang, Xiaofei Tan, Guangming Zeng, Xinjiang Hu, Zhongzhu Yang

College of Environmental Science and Engineering, Hunan University, Changsha 410082, PR China
Key Laboratory of Environmental Biology and Pollution Control (Hunan University), Ministry of Education, Changsha 410082, PR China

ARTICLE INFO

Article history:
Received 30 April 2014
Accepted 25 July 2014
Available online 4 August 2014

Keywords:
Modified ramie fiber
Adsorption
Heavy metals
EGTA dianhydride
Mercerization
Adsorption isotherm
Regeneration

ABSTRACT

In this study, the removal of Cd^{2+} and Pb^{2+} from aqueous solutions was investigated using a novel chelating material. The first part described the synthesis of ethylene glycol-bis(2-aminoethylether)-N,N,N′,N′-tetraacetic acid dianhydride (EGTAD), mercerization treatment of ramie fiber (MRF), and the MRF was then reacted with EGTAD to prepare the new material (ERF). The obtained material was characterized by weight gain, SEM, FTIR, and elemental analysis. The results of FTIR and elemental analysis confirmed that ester bond, carboxyl and amine groups were introduced onto ERF. The adsorption capacity of metals on ERF was evaluated at different contact times, pH values, initial metal concentrations, and temperatures in the second part. The adsorption equilibrium was reached within 5 min for Cd^{2+} and Pb^{2+}. Adsorption isotherm could be well fitted by the Langmuir model, and the maximum adsorption capacities were 159.11 and 273.78 mg g^{-1} for Cd^{2+} and Pb^{2+} at 298 K, respectively. Thermodynamic analysis showed that the adsorption process was spontaneous and endothermic. The molar ratio of adsorbed cation to grafted EGTA is close to 1.8:1, which confirmed that the adsorption was chemical process involving both surface chelation reaction and ion exchange. In addition, the absorbent was successfully regenerated using HCl and ultrasonic treatment.

1. Introduction

The heavy metals in water could be mainly derived from mining, industrial discharges and particulates in the atmosphere. Cadmium is associated with bone and kidney damage at long-term exposure [1]. Lead causes brain damage, kidney and liver disorders and toxicity to the reproductive system [2,3]. Various methods were employed for the removal of heavy metal ions from aqueous solution, including chemical precipitation, ion exchange, coagulation, membrane separation, electrolytic reduction and adsorption [4,5]. Adsorption has been proved as one of the most efficient and technically feasible methods for the removal of heavy metals from aqueous solutions [6]. Activated carbon has been the most widely applied adsorbent throughout the world. However, the applications of activated carbon are restricted due to its high operating costs and difficult regeneration.

Cellulose is considered as the most abundant and renewable polymer resource worldwide [1]. Ramie (*Boehmeria nivea*) is widely planted in Asian countries such as China, Philippines, India, and Thailand [7]. Ramie fiber, stripped from stem bast of the plant, is considered to be the longest, strongest, and silkiest plant fiber [8], and the content of cellulose is relatively high (68.6–76.2 wt.%) [7]. Therefore, ramie fiber is mainly used for textile material, industrial pack-aging, canvas, car outfits, etc. Besides, the application of natural cellulose as adsorbent has received more attention in recent years.

It is recognized that cellulose is a linear macromolecule formed by β-d anhydroglucose units and linked together by 1,4-glucosidic bonds [7]. Cellulose chains are able to form intra- and inter-molecular hydrogen bonds, leading to organized chain structure. Thus ramie fiber can be regarded as a highly crystalline fiber and the further exploitation and utilization of ramie products are restricted by their high degree of crystallization and orientation [9]. Therefore, seeking effective modified methods to overcome these disadvantages has become very important.

In order to maximize the removal of heavy metals from aqueous solution, it is important that metals strongly bind on the adsorbent's surface. It was reported that chelating agents such as aminopolycarboxylic acids form stable structures with metal ions. Ethylene glycol-bis(2-aminoethylether)-N,N,N′,N′-tetraacetic acid (EGTA) is a powerful chelating agent, which has a greater selective preference for larger divalent metal ions than EDTA [10]. Treatment of lignocellulosic materials with an aqueous NaOH solution could lead to an increase in internal surface area, a decrease in

* Corresponding author at: College of Environmental Science and Engineering, Hunan University, Changsha 410082, PR China. Fax: +86 731 88823701.
E-mail address: liuyunguo@hnu.edu.cn (Y. Liu).

http://dx.doi.org/10.1016/j.jcis.2014.07.036
0021-9797/

crystallinity, the separation of the structural linkages between lignin and carbohydrates and disruption of the lignin structure [11]. Therefore, mercerization treatment is a way to increase the fibers specific surface area and to make the hydroxyl groups of cellulose macromolecules more easily accessible for the introduction of EDTA dianhydride (EGTAD) [12].

To the best of our knowledge, the use of ramie fiber or modified ramie fiber on the adsorption of heavy metals in water has rarely reported. And EGTA was rarely reported as a modifier, and the only materials modified with EGTA in the available literatures and patents are polymer membrane and chitosan [6,13]. In addition, there are few reports concerned with the synthesis of EGTAD and the modification of ramie with EGTAD. In this study, mercerized ramie fiber is chemically modified with EGTAD. This reaction allowed the introduction of carboxylic and amine groups to the ramie fiber via the formation of ester functions. The adsorption capacity of metals on EGTAD modified ramie fiber (ERF) was evaluated at different contact times, pH values, initial metal concentrations, and temperatures. In order to examine the mechanism of adsorption, the kinetics, adsorption isotherms, and thermodynamics analysis were evaluated.

2. Materials and methods

2.1. Materials

The ramie fiber was produced in Hunan province of China. EGTA (Aladdin-reagent) was used without further purification. Acetic anhydride (Ac_2O), N,N′-dimethyl formamide (DMF), sodium hydroxide (NaOH), acetone, diethylether, sodium hydrogen carbonate ($NaHCO_3$), pyridine, ethanol, n-hexane, ethyl alcohol, $Cd(NO_3)_2{\cdot}4H_2O$, $Pb(NO_3)_2$ and nitric acid were purchased from local chemical suppliers and used without any treatment. Milli-Q ultrapure water (18.2 MΩ cm) was used throughout the study.

2.2. Preparation of ramie fiber and EGTA anhydride (EGTAD)

After being stripped from the stem bast of ramie, the ramie fiber was dried at 80 °C in an oven for 24 h and then the fiber was cut to 100–150 μm by a grinder. The material was then washed with ultrapure water and dried at 65 °C for 2 h.

EGTAD was synthesized following the method described elsewhere with revision [14,15]. 23.0 g EGTA (0.060 mol) was suspended in 30.0 mL anhydrous pyridine and 15.0 mL anhydrous DMF. Then 25.0 mL acetic anhydride was added dropwise. The mixtures were agitated strongly at 65 °C for 24 h and then filtered, washed with acetic anhydride, diethyl ether, and dried under vacuum at 60 °C for 2 h.

2.3. Mercerization and modification of ramie fiber

10.0 g ramie fiber (RF) was dispersed in 60.0 mL n-hexane at 50 °C for 3 h to remove the botanic wax, and the dewaxed ramie fiber was treated with 500.0 mL NaOH solution (4.0 mol L^{-1}) at 25 °C under stirring for 24 h. Then the fibers were filtered, and washed with plenty of ultrapure water, ethanol, and acetone. Mercerized ramie fiber (MRF) was dried in an oven at 65 °C for 3 h and left to cool in a desiccator.

5.0 g MRF and 10.0 g EGTAD were suspended in 50.0 mL DMF and 20.0 mL pyridine. The mixture was stirred at 75 °C for 20 h. After filtration, the obtained new materials (ERF) were washed with DMF, ultrapure water, saturated sodium bicarbonate solution, ultrapure water, ethanol 95%, acetone, and then dried in an vacuum for 3 h at 60 °C and left to cool in a desiccator.

2.4. Characterization of RF, MRF, and ERF

The morphology of the materials was studied by FEI QUANTA 200 environmental scanning electron microscopy. Infrared spectra were obtained from the Fourier transform infrared spectrophotometer (Nico-let, Nexus-670 FTIR). Elemental analyses were carried out with an Elementar Vario ELIII elemental analyzer (Germany). The loading of EGTA on ERF was deduced from Eq. (1):

$$W_{ERF} = W_E \times \%\mathrm{EGTA} + W_{MRF} \times (1 - \%EGTA) \quad (1)$$

where W_{ERF}, W_E and W_{MRF} are the nitrogen content of ERF, EGTA and MRF, respectively; %EGTA is the content of the EGTA group in ERF.

2.5. Batch adsorption studies

2.5.1. Kinetic study of metal ion adsorption for ERF

An amount of 50.0 mg of adsorbent was placed in a 150 mL Erlenmeyer flask with 50.0 mL of metal ion solution at fixed concentrations (200 mg L^{-1} for Cd^{2+} and 200 mg L^{-1} for Pb^{2+}), at pH 4.5 for Cd^{2+} and 4.0 for Pb^{2+}, respectively. The pH values were measured during the experiment. The Erlenmeyer flasks were shaken at a constant speed (150 rpm) at 25 °C for different time intervals (1, 3, 5, 10, 20, 40, 60, 90 and 120 min). At the end of the experiment, the samples were centrifuged at 4000 rpm for 10 min, the metal ion concentrations were determined using an atomic absorption spectrophotometer (Analyst 700, Perkin Elmer, America). The adsorption amount q_e (mg g^{-1}) was calculated according to Eq. (2):

$$q_e = \frac{(C_0 - C_e) \times V_m}{m} \quad (2)$$

where C_0 and C_e (mg L^{-1}) are the initial and equilibrium metal ions concentration, respectively. V_m (mL) is the volume of the metal ion solution, and m (mg) is the mass of adsorbent.

2.5.2. Effect of pH on metal ion adsorption onto ERF

An amount of 50.0 mg of adsorbent was placed in a 150 mL Erlenmeyer flask with 50.0 mL of metal ion solution at fixed concentrations (200 mg L^{-1} for Cd^{2+} and 200 mg L^{-1} for Pb^{2+}). The pH range studied for ERF was from 2.5 to 7.0 for Cd^{2+} and 1.5 to 6.5 for Pb^{2+}, respectively. The pH values were adjusted by the addition of drops of aqueous HCl or NaOH solutions (0.01–1.0 mol L^{-1}). The Erlenmeyer flasks were shaken at a constant speed (150 rpm) at 25 °C for 60 min. At the end of the experiment, the samples were centrifuged at 4000 rpm for 10 min, and the metal ion concentrations were determined as described earlier.

2.5.3. Adsorption isotherms of RF and ERF

An amount of 50.0 mg of adsorbent was placed in a 150 mL Erlenmeyer flask with 50.0 mL of metal ion solution at fixed concentrations (20–500 mg L^{-1} for Cd^{2+}, and 20–600 mg L^{-1} for Pb^{2+}), at pH value of 4.0. The pH values were measured during the experiment. The Erlenmeyer flasks were shaken at a constant speed (150 rpm) at different temperatures (25, 30 and 40 °C) for 60 min. At the end of the experiment, the samples were centrifuged at 4000 rpm for 10 min, and the metal ion concentrations were determined as described earlier.

2.6. Regeneration studies

Regeneration experiment was investigated to evaluate the reusability of the material. An amount of 100.0 mg of adsorbent was placed in a 150 mL Erlenmeyer flask with 100.0 mL of metal ion solution at fixed concentrations (200 mg L^{-1} for Cd^{2+} and 200 mg L^{-1} for Pb^{2+}). After attaining equilibrium, the spent adsorbent was separated

from the solution by centrifugation and filtration. Metal ions were eluted using 0.5 M of 100.0 mL hydrochloric acid (HCl) only or both 0.5 M HCl and 20 s ultrasonic treatments. The eluted adsorbent was then placed in 150 mL Erlenmeyer flask with 100.0 mL of ultrapure water, and the flask was transferred into an ultrasound generator (KQ-500E, Kunshan Ultrasound Instrument Co., Ltd.) operating at 50 kHz with a power of 150 W (25 °C). After each cycle of adsorption–desorption, absorbents were washed with distilled water and reused in the succeeding cycle. The adsorption–desorption cycles were repeated consecutively ten times to determine the reusability of sorbents.

3. Results and discussion

3.1. Characterization of RF, MRF, and ERF

3.1.1. SEM characterization of RF, MRF, and ERF

The surface morphologies of RF, MRF, and ERF are shown in Fig. 1. The ramie fiber had a relatively smooth and compact surface with some particle matter (Fig. 1a and b). After treatment with an aqueous NaOH solution (4 mol L^{-1}), the ramie fiber of cylindrical shape shrinked dramatically (Fig. 1d), and the surface of ramie fiber became concave (Fig. 1c). The probable reason was that mercerized treatment could solubilize lignin and hemicellulose [16]. The surface of ERF appeared some silk-like materials and the granular substance was disappeared compared to the MRF and RF (Fig. 1e and f), which was possibly due to the chemical modification with EGTAD.

3.1.2. FTIR analysis

Fig. 2 shows the FTIR spectra of RF, MRF and ERF. The major change noticed in FTIR spectra of ERF was the arising of a strong band at 1742 cm^{-1} when compared to RF and MRF, which was corresponding to asymmetric and symmetric stretching of C–O. The new peak confirmed that ester bond and carboxyl were introduced onto ERF after modification with EGTAD. The unchanged absorption bands of RF at 3433, 1638, 1060 cm^{-1} suggested that the main structure of the fiber remained after chemical modification. The self-consistent band at 3433 cm^{-1} was due to the stretching of hydroxyl groups, because only the surface hydroxyls were accessible to EGTAD during the esterification reaction. The slight decrease in the 887 cm^{-1} band of MRF was characteristic of β-linked

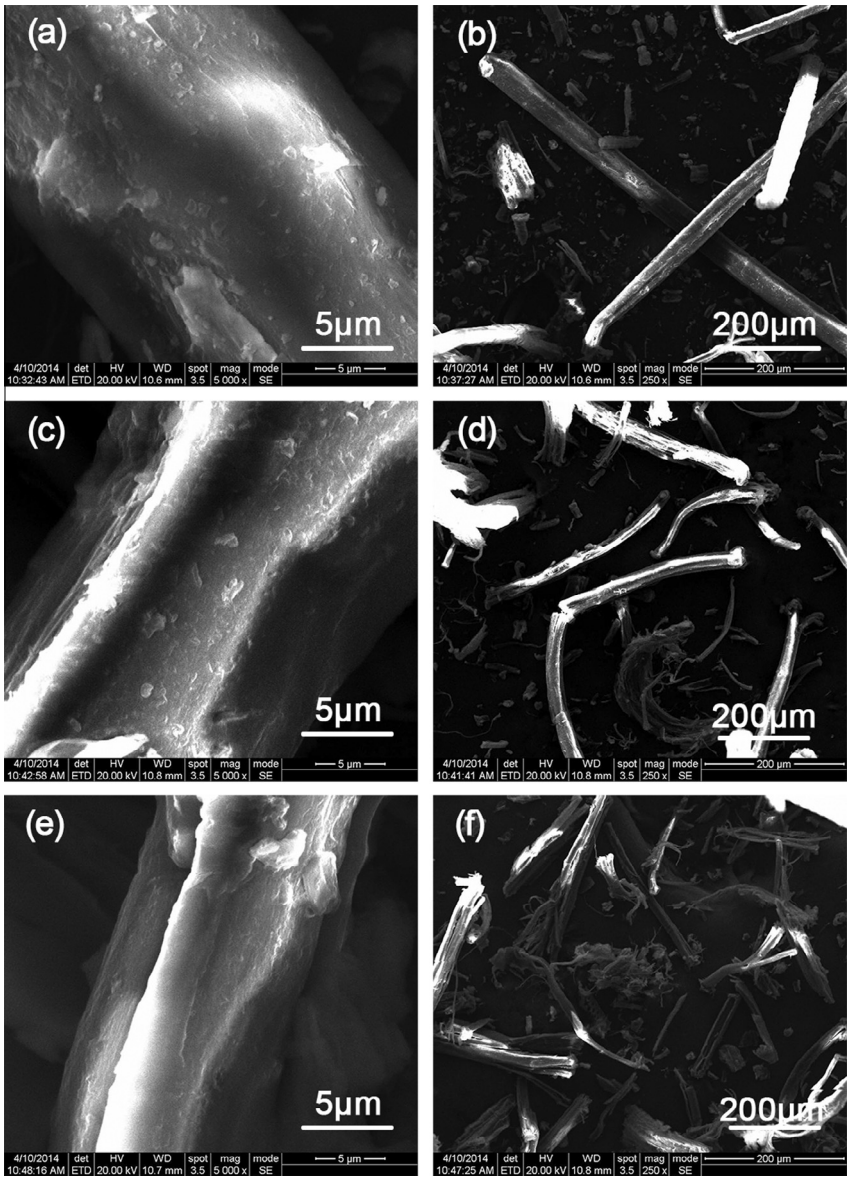

Fig. 1. SEM images of RF (a and b), MRF (c and d) and ERF (e and f).

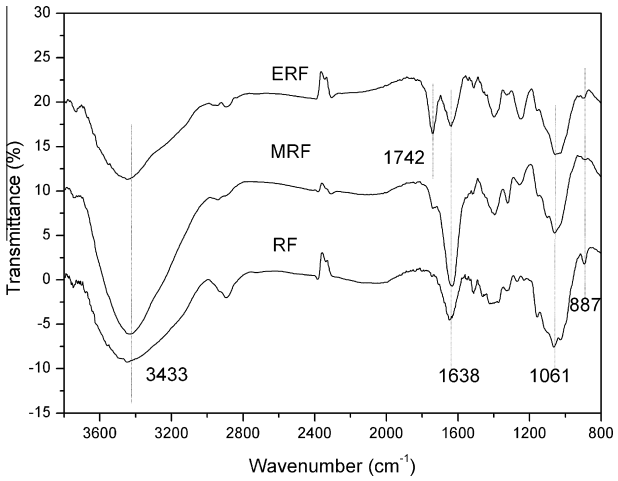

Fig. 2. FTIR spectra of RF, MRF and ERF.

hemicelluloses [17]. Previous study reported that NaOH solution (above 17.5%) could solubilize β- and γ-cellulose which had lower degree of polymerization than α-cellulose [12].

3.1.3. Synthesis of ERF and elemental analysis

The synthesis route of ERF and suggested mechanism for the adsorption of metal ions are shown in Fig. 3. The reaction between hydroxyl groups of materials and EGTAD allowed the introduction of carboxylic and amine functional groups to the materials through formation of ester linkage [18]. Compared to RF, MRF exhibited a decrease of 20.56% in the mass percent gain. And ERF exhibited an increase of 22.5% in the mass percent gain with respect to MRF. The elemental analyses results are presented in Table 1. The higher nitrogen content of ERF proved the introduction of the EGTD. The introduced EGTA-group was calculated from the difference between the nitrogen content of MRF (2.233%), ERF (1.035%), and EGTA (7.36%) by using Eq. (1). The calculated result showed that the content of the EGTA-group in ERF was 0.777 mmol g^{-1}. According to this result, the theoretical mass percent gain of ERF was 41.9%, but the practical mass percent gain of it was only 22.5% in the experiment. This is probably due to the loss of MRF during the synthesis and purification procedures.

3.2. Adsorption studies

3.2.1. Kinetic studies

Cd^{2+} and Pb^{2+} removal by the new adsorbent as a function of contact time is shown in Fig. 4a. The adsorption of Cd^{2+} and Pb^{2+} sharply increased during the first minute, with more than 95% of the total ions being adsorbed by the ERF, which was due to the presence of numerous active sites on the adsorbent surface. Then the amount of metals adsorbed increased slowly and approached equilibrium was reached within 5 min for Cd^{2+} and Pb^{2+}. It could be explained by the fact that a lot of active surface sites were occupied by metal ions and the remaining active surface sites were difficult to be occupied due to repulsive forces between the molecules [19].

To investigate the rate of the adsorption and the rate-controlling step of the adsorption process such as chemical reaction, Pseudo-second-kinetic model was used to analyze the experimental data.

$$\frac{t}{q_t} = \frac{1}{kq_e^2} + \frac{t}{q_e} \tag{3}$$

$$h = kq_e^2 \tag{4}$$

where k (g mg^{-1} min^{-1}) is the adsorption rate constant of the pseudo-second-order, q_t represents the amount of metals adsorbed at time t (min), q_e (mg g^{-1}) is the adsorption capacity calculated by

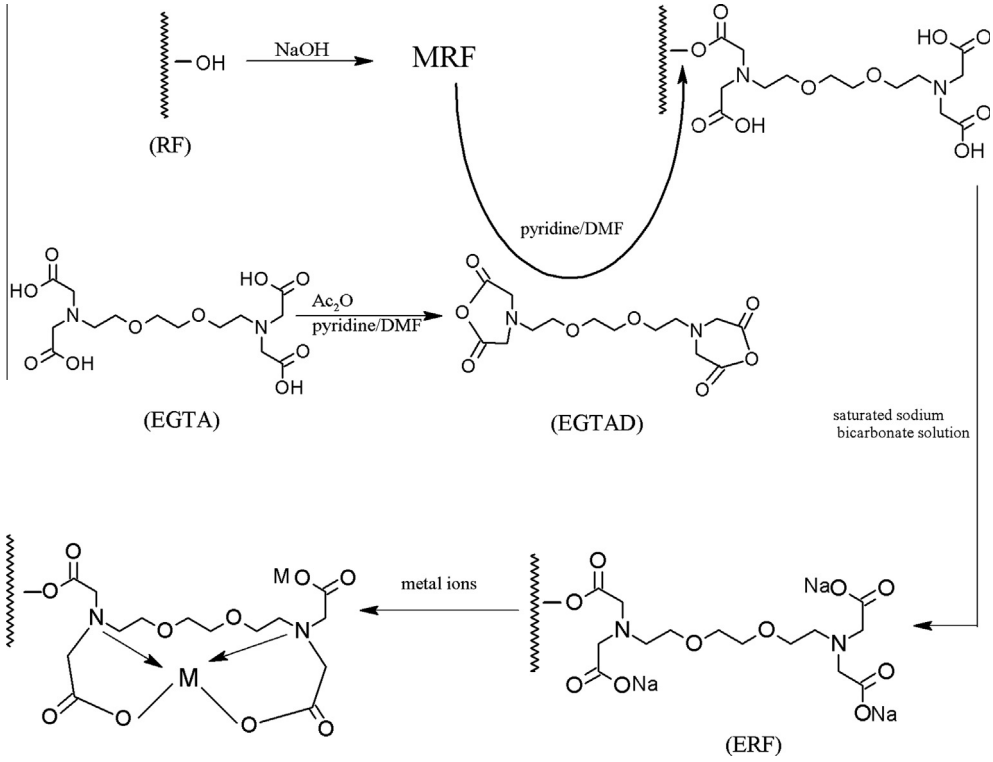

Fig. 3. The synthesis route to ERF and suggested mechanism for the adsorption of metal ions.

Table 1
Results of elemental analysis for RF, MRF and ERF.

Sample	Elemental content (wt.%)			%EGTA (wt.%)	Loading of EGTA (mmol g^{-1})
	C	H	N		
RF	40.61	6.390	1.035	0	0
MRF	42.22	7.241	0.081	0	0
ERF	43.02	6.699	2.233	29.56	0.777

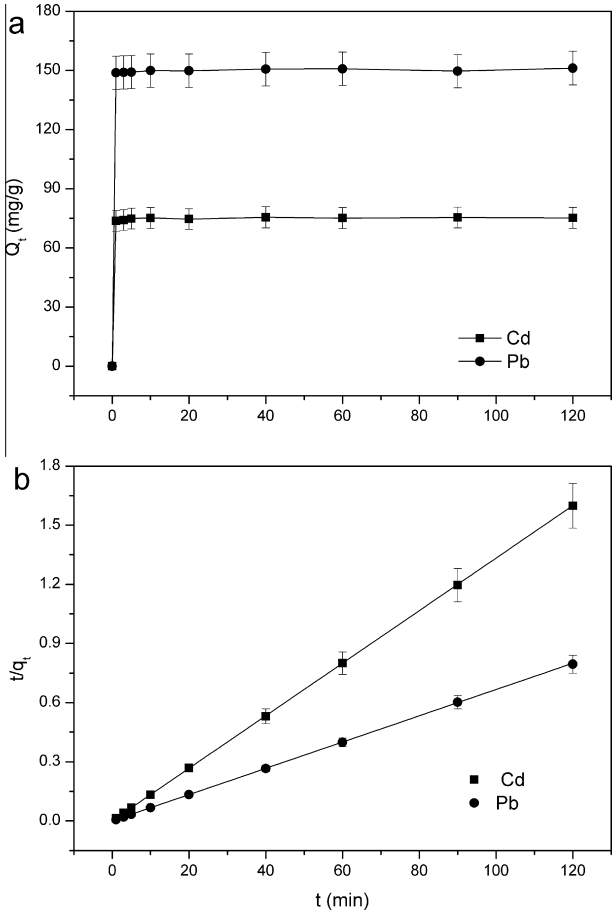

Fig. 4. Effects of contact time on Cd^{2+} and Pb^{2+} adsorption capacity (a); linear fit of experimental data for pseudo-second-order adsorption kinetic model (b).

the pseudo-second-order kinetic model, h (mg g^{-1} min^{-1}) is the initial adsorption rate.

According to Fig. 4b and Table 2, the calculated q_e values agreed very well with the experimental data, and the correlation coefficients were more than 0.9999. This result indicates that the kinetic data were well fitted to the pseudo-second order model, implying that the adsorption mechanism depended on the adsorbate and adsorbent, and the rate-controlling step might be a chemical sorption involving ion exchange or surface chelation reaction as suggested in Fig. 3 [6]. The initial adsorption rate (h) of Cd^{2+} and Pb^{2+} are 3397.17 and 12399.20 mg g^{-1} min^{-1}, respectively, suggesting an initial fast adsorption process.

3.2.2. Effect of pH

The effect of pH on Cd^{2+} and Pb^{2+} adsorption by ERF is presented in Fig. 5. The solution pH influenced on the adsorption because it affects the activity of functional groups (carboxyl, amine groups), as well as the competition of metal ions for the free binding sites. The adsorption capacity increased with the increasing of pH values and reached a maximum at pH approximately 5.5 for Cd^{2+} and Pb^{2+}. At lower pH values, functional groups of ERF were closely associated with hydronium ions (H_3O^+) and restricted the approach of metals as a result of the repulsive force. While the pH increased, the adsorption surface became deprotonated, thus increasing the amount of metals adsorbed [20]. The amount of Pb^{2+} adsorbed on ERF decreased at pH above 5, possibly due to the formation of metallic precipitation. Over the pH range from 2.5 to 5.5, the adsorption capacities for Cd^{2+} and Pb^{2+} decreased slowly from 68.6 and 174.1 mg g^{-1} to 46.5 and 140.3 mg g^{-1}, respectively. Some literatures reported that the adsorption capacity decreased dramatically with the decrease of pH values [20,21]. Compared with these results, the adsorption capacity of ERF was changed little over the pH range from 5.5 to 2.5, which indicating that the complex between metal ions and the carboxyl and amine groups of the adsorbent was stable.

3.2.3. Adsorption isotherm

Adsorption isotherms describe how adsorbates interact with adsorbents. The maximum adsorption amount of Cd^{2+} and Pb^{2+} for ERF at 298 K, 313 K and 328 K are shown in Fig. 6. Two important and typical isotherms were used to evaluate the equilibrium results: Constants and correlation regression coefficients of Cd^{2+} and Pb^{2+} adsorption are presented in Table 3.

As an empirical equation, model is more suitable for heterogenous adsorption, which is not restricted to the formation of a monolayer [22]. The Freundlich model is given by the following equation [23]:

$$q_e = K_f c_e^{\frac{1}{n}} \tag{5}$$

where q_e (mg g^{-1}) is the adsorption capacity at equilibrium concentration, c_e (mg L^{-1}) is the equilibrium solute concentration, K_f and n are the Freundlich constants.

The Freundlich model did not fit the experimental data well (Table 3). In this study, n values were all higher than 1, which implied that adsorption intensity was favorable at high concentrations but much less at lower concentrations [24].

The Langmuir isotherm theory assumes monolayer coverage of adsorbate on a homogeneous surface of adsorbent [22]. This model can be expressed by the following equation [25]:

$$q_e = \frac{K_L q_m c_e}{1 + K_L c_e} \tag{6}$$

$$R_L = \frac{1}{1 + K_L c_0} \tag{7}$$

where q_m (mg g^{-1}) is the maximum adsorption capacity, c_e (mg L^{-1}) is the equilibrium solute concentration, K_L (L mg^{-1}) is the Langmuir constant related to adsorption energy, c_0 (mg L^{-1}) is the initial concentration of Cd^{2+} and Pb^{2+}, R_L is the equilibrium parameter which can be applied to predict whether the adsorption is favorable.

It was obvious from Fig. 6 that temperature of 313 K showed the highest capacity for Cd^{2+} and Pb^{2+} adsorption by the adsorbents. Maximum adsorption capacity q_m was calculated to be 185.63 and 294.58 mg g^{-1} for Cd^{2+} and Pb^{2+} (Table 3). The Langmuir isotherm model was appropriate for the results with the higher

Table 2
Pseudo-second-order kinetics constants for metal ions onto ERF.

Metal	Pseudo-second-order constants				
	$q_{e,exp}$ (mg g^{-1})	q_e (mg g^{-1})	k (g mg^{-1} min^{-1})	h (mg g^{-1} min^{-1})	R^2
Cd^{2+}	74.82	75.02	0.60362	3397.17	0.99998
Pb^{2+}	149.35	149.93	0.55159	12399.20	0.99998

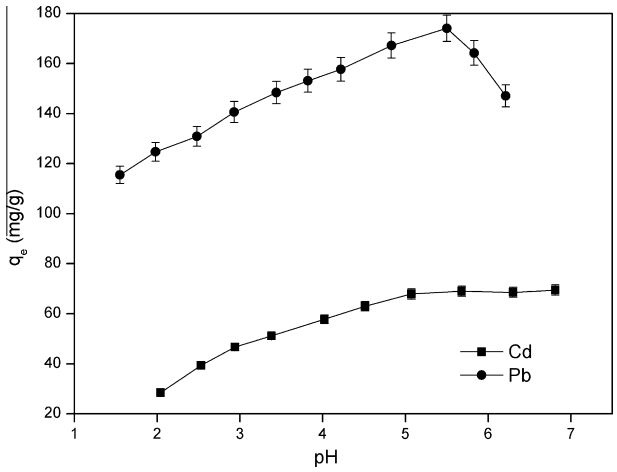

Fig. 5. Effects of pH on Cd^{2+} and Pb^{2+} adsorption by ERF.

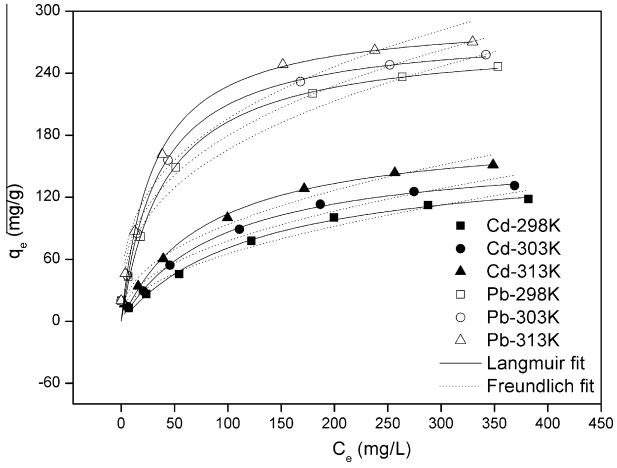

Fig. 6. Adsorption isotherms for Cd^{2+} and Pb^{2+} onto ERF at various temperatures.

correlation coefficient R^2. In addition, the stability constant (K_L) increased with the increase of temperature, indicating that the bond energy between the surface sites and metal ions was larger at higher temperature [20]. The K_L values in this study were calculated in the range from 0.047 to 0.861, indicating that the adsorption between metal ions and adsorbent was favorable ($0 < K_L < 1$) [3,26].

3.2.4. Thermodynamic analysis

Temperature was of great importance for energy-dependent mechanism in metal adsorption. Therefore, thermodynamic analysis was taken to gain further insights into sorption process and mechanisms. Thermodynamic parameters such as Gibbs free energy ΔG^0, enthalpy ΔH^0, entropy ΔS^0 were calculated by the following equations [27]:

$$\Delta G^0 = -RT\ln K \tag{8}$$

$$\ln K = -\frac{\Delta G^0}{RT} = -\frac{\Delta H^0}{RT} + \frac{\Delta S^0}{R} \tag{9}$$

where the gas constant R is 8.314 J mol^{-1} K^{-1}, T is the absolute temperature (K), K is the equilibrium constant, which can be obtained from Langmuir isotherms at different temperature. ΔH^0 and ΔS^0 could be calculated from the slope and intercept of $\ln K$ versus $1/T$. Thermodynamic analysis was investigated at three different temperatures (298, 303 and 313 K). The calculated results are given in Table 4.

The negative values of ΔG^0 indicated the spontaneous nature of the adsorption. For an increase in the range of temperatures from 298 to 313 K, the ΔG° values became more negative suggesting that the adsorption was more favorable at high temperature. Moreover, the positive values of ΔH^0 verified that the endothermic nature of sorption and further supported by the increase of sorption capacity with the increase in temperature. Finally, the positive values of ΔS^0 might be attributed to the increasing randomness during the adsorption process.

3.2.5. Adsorption mechanism

The surface of EGTAD and sodium bicarbonate solution treated ramie fiber contained carboxylic and amine functional groups. The metal was coordinated via 2 carboxyl groups and 2 amine nitrogen, and the remaining carboxyl group could adsorb metal by ion exchange (Fig. 3). Simple calculations showed that the maximum adsorption capacities of ERF were 1.416 and 1.321 mmol g^{-1} for Cd^{2+} and Pb^{2+} at 298 K, respectively (Table 3), and the content of the EGTA-group introduced to the surface of ERF was 0.777 mmol g^{-1} (Table 2). These results demonstrated that the ratio between the amount of Cd or Pb adsorbed and that of introduced EGTA were close to 1.8:1, which confirmed that the adsorption was a chemical process involving both surface chelation reaction and ion exchange.

Table 3
Isotherm constants for metal ions onto ERF at various temperatures.

Metal	T (K)	Langmuir model				Freundlich model		
		q_m (mg g^{-1})	K_L (L mg^{-1})	R_L	R^2	K_f (L mg^{-1})	n	R^2
Cd^{2+}	298	159.11	0.008	0.199–0.861	0.996	6.628	2.015	0.973
	303	166.18	0.011	0.156–0.822	0.997	9.393	2.180	0.966
	313	185.63	0.013	0.136–0.797	0.991	12.725	2.306	0.977
Pb^{2+}	298	273.78	0.024	0.065–0.677	0.990	31.578	2.775	0.958
	303	281.70	0.029	0.054–0.633	0.991	36.667	2.899	0.953
	313	294.58	0.034	0.047–0.596	0.990	42.868	3.030	0.950

Table 4
Thermodynamic parameters for the adsorption of metal ions onto ERF at various temperatures.

Metal	T (K)	ΔG^0 (kJ mol^{-1})	ΔS^0 (J mol^{-1} K^{-1})	ΔH^0 (kJ mol^{-1})	R^2
Cd^{2+}	298	−0.248	21.750	6.251	0.994
	303	−0.341			
	313	−0.560			
Pb^{2+}	298	−1.753	56.880	15.292	0.998
	303	−1.994			
	313	−2.519			

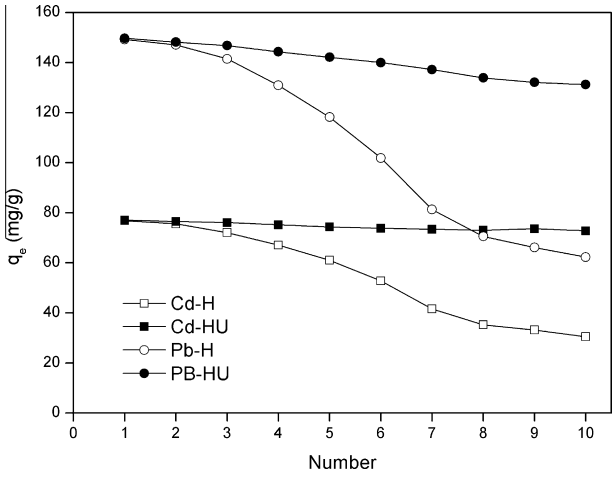

Fig. 7. Ten consecutive adsorption–desorption cycles of ERF for Cd^{2+} and Pb^{2+}. (H represents HCl treatment and U represents ultrasonic treatment.)

3.3. Regeneration studies

Desorption was carried out with HCl only or HCl combined with ultrasonic treatment. The regenerated ERF was reused for up to 10 adsorption–desorption cycles and the results are shown in Fig. 7. It was found that the adsorption capacity of the ERF decreased from 76.8 to 30.5 mg g^{-1} for Cd^{2+} and from 149.7 to 61.3 mg g^{-1} for Pb^{2+}, respectively, after ten cycle of regeneration. However, the 20 s ultrasonic treatments after HCl could effectively regenerate the adsorbent with regeneration efficiencies ranging from 95% to 99%. The probable reason was that ultrasonic treatment increased the free spaces for the metal ions on the surface of adsorbent. These results showed that the ERF could be successfully regenerated by HCl and ultrasonic treatment.

4. Conclusions

EGTAD modified ramie fiber, as a novel material, was found to effectively absorb Cd^{2+} and Pb^{2+} from aqueous single metal solutions. The higher content of nitrogen for elemental analyses and the arising of a strong band at 1742 cm^{-1} for FTIR analyses confirmed that ester bond, carboxyl and amine groups were introduced onto ERF after modification with EGTAD. The adsorption equilibrium was reached within 5 min for Cd^{2+} and Pb^{2+}, and the maximum adsorption capacities were 159.11 and 273.78 mg g^{-1} for Cd^{2+} and Pb^{2+} at 298 K, respectively. Pseudo-second-order and Langmuir model described the adsorption processes well, implying that the adsorption processes might be a chemical sorption. Thermodynamic analysis showed that the adsorption process was spontaneous and endothermic. What is more, the adsorption capacity was changed little over the pH range 5.5–2.5, and the regeneration efficiency of EFR was varied from 95% to 99% after HCl and ultrasonic treatment. On the whole, the effective and environmental friendly absorbent showed its potential to be applied in the removal of heavy metal ions from polluted water.

Acknowledgments

This work was supported by the National Natural Science Foundation of China (Grant No. 41271332), the Science and Technology Planning Project of Hunan Province, China (Grant No. 2012SK2021), and the Hunan Provincial Innovation Foundation For Postgraduate (Grant No. CX2012B138).

References

[1] D.W. O'Connell, C. Birkinshaw, T.F. O'Dwyer, Bioresour. Technol. 99 (2008) 6709–6724.
[2] E. Repo, J.K. Warchoł, A. Bhatnagar, M. Sillanpää, J. Colloid Interface Sci. 358 (2011) 261–267.
[3] W. Shao, L. Chen, L. Lü, F. Luo, Desalination 265 (2011) 177–183.
[4] S. Hokkanen, E. Repo, M. Sillanpää, Chem. Eng. J. 223 (2013) 40.
[5] E. Repo, R. Koivula, R. Harjula, M. Sillanpää, Desalination 321 (2013) 93.
[6] F. Zhao, E. Repo, D. Yin, M.E. Sillanpää, J. Colloid Interface Sci. 409 (2013) 174–182.
[7] Z.T. Liu, Y. Yang, L. Zhang, P. Sun, Z.W. Liu, J. Lu, H. Xiong, Y. Peng, S. Tang, Carbohydr. Polym. 71 (2008) 18–25.
[8] S. Basu, M.N. Saha, D. Chattopadhyay, K. Chakrabarti, J. Ind. Microbiol. Biotechnol. 36 (2009) 239–245.
[9] Z.T. Liu, X. Fan, J. Wu, L. Zhang, L. Song, Z. Gao, W. Dong, H. Xiong, Y. Peng, S. Tang, React. Funct. Polym. 67 (2007) 104–112.
[10] S. Hegde, S. Kapoor, S. Joshi, T. Mukherjee, Colloids Surf., A 280 (2006) 116–124.
[11] S. Min, J. Han, E. Shin, J. Park, Water Res. 38 (2004) 1289–1295.
[12] O.K. Júnior, L.V.A. Gurgel, R.P. de Freitas, L.F. Gil, Carbohydr. Polym. 77 (2009) 643–650.
[13] R.L. Bruening, K.E. Krakowiak, A.J. DiLeo, T. Jiang, Google Pat. (2004).
[14] A. Capretta, R.B. Maharajh, R.A. Bell, Carbohydr. Res. 267 (1995) 49–63.
[15] L.R. Chervu, B. Sundoro, M.D. Blaufox, J. Nucl. Med. 25 (1984) 1111–1115.
[16] D. Klemm, B. Heublein, H.P. Fink, A. Bohn, Angew. Chem., Int. Ed. 44 (2005) 3358–3393.
[17] R. Sun, J. Fang, L. Mott, J. Bolton, Holzforschung 53 (1999) 253–260.
[18] J. Yu, M. Tong, X. Sun, B. Li, Bioresour. Technol. 99 (2008) 2588–2593.
[19] I. Mall, V. Srivastava, G. Kumar, I. Mishra, Colloids Surf., A 278 (2006) 175–187.
[20] L.V.A. Gurgel, L.F. Gil, Water Res. 43 (2009) 4479–4488.
[21] S. Hokkanen, E. Repo, T. Suopajärvi, H. Liimatainen, J. Niinimaa, M. Sillanpää, Cellulose (2014) 1–17.
[22] K.A. Guimarães Gusmão, L.V. Alves Gurgel, T.M. Sacramento Melo, L.F. Gil, Dyes Pigm. 92 (2012) 967–974.
[23] S. Chen, Q. Yue, B. Gao, Q. Li, X. Xu, Chem. Eng. J. 168 (2011) 909–917.
[24] Y.S. Al-Degs, M.I. El-Barghouthi, A.A. Issa, M.A. Khraisheh, G.M. Walker, Water Res. 40 (2006) 2645–2658.
[25] X.J. Hu, J.S. Wang, Y.G. Liu, X. Li, G.M. Zeng, Z.L. Bao, X.X. Zeng, A.W. Chen, F. Long, J. Hazard. Mater. 185 (2011) 306–314.
[26] K. Hall, L. Eagleton, A. Acrivos, T. Vermeulen, Ind. Eng. Chem. Fundam. 5 (1966) 212–223.
[27] Z.Y. Yao, J.H. Qi, L.H. Wang, J. Hazard. Mater. 174 (2010) 137–143.